

Evolution and Functional Characterization of the *RH50* Gene from the Ammonia-Oxidizing Bacterium *Nitrosomonas europaea*^{∇†}

Baya Cherif-Zahar,^{1,2} Anne Durand,³ Ingo Schmidt,⁴ Nabila Hamdaoui,^{1,2} Ivan Matic,^{2,5} Mike Merrick,³ and Giorgio Matassi^{6*}

INSERM, U845, Paris F-75015, France¹; Université Paris Descartes, Faculté de Médecine René Descartes, Paris F-75015, France²; Department of Molecular Microbiology, John Innes Centre, Colney Lane, Norwich NR4 7UH, United Kingdom³; Department of Microbiology, University of Bayreuth, Universitaetsstrasse 30, 95447 Bayreuth, Germany⁴; INSERM, U571, Paris F-75015, France⁵; and Institut Jacques Monod, CNRS-UMR 7592, Université Paris 6 et Paris 7, 2 Place Jussieu, 75251 Cedex 05, Paris, France⁶

Received 10 July 2007/Accepted 4 September 2007

The family of ammonia and ammonium channel proteins comprises the Amt proteins, which are present in all three domains of life with the notable exception of vertebrates, and the homologous Rh proteins (Rh50 and Rh30) that have been described thus far only in eukaryotes. The existence of an *RH50* gene in bacteria was first revealed by the genome sequencing of the ammonia-oxidizing bacterium *Nitrosomonas europaea*. Here we have used a phylogenetic approach to study the evolution of the *N. europaea* *RH50* gene, and we show that this gene, probably as a component of an integron cassette, has been transferred to the *N. europaea* genome by horizontal gene transfer. In addition, by functionally characterizing the Rh50_{Ne} protein and the corresponding knockout mutant, we determined that NeRh50 can mediate ammonium uptake. The *RH50*_{Ne} gene may thus have replaced functionally the *AMT* gene, which is missing in the genome of *N. europaea* and may be regarded as a case of nonorthologous gene displacement.

Since the first description of rhesus (Rh) antigens in 1940 by Landsteiner and Wiener (45), the Rh blood group has become, after the ABO group, the most clinically significant in transfusion medicine. It is the most polymorphic of human blood groups, consisting of at least 45 independent antigens, and is consequently also widely used in human population genetics studies. In humans, Rh antigens are carried by two erythrocyte membrane proteins, named RhD and RhCE, and are also referred to as Rh30 because of their apparent molecular mass of 30 to 32 kDa. These proteins are coded by two very similar paralogous genes (ca. 96% identical at the nucleotide level), located in tandem on chromosome 1p34-36. The human genome also codes for three other members of the Rh family, the Rh50 transmembrane glycoproteins (Rh50A/RhAG, Rh50B/RhBG, and Rh50C/RhCG) that have an apparent molecular mass of 50 to 58 kDa (6). The Rh50A protein is erythroid specific, like Rh30, and is associated with Rh30 in a multiprotein complex in the red blood cell membrane (10). Rh50A expression is required for Rh blood group antigen expression at the red blood cell membrane (14), and its lack of expression results in the Rh-null phenotype (68). In mammals, the nonerythroid Rh50B and Rh50C proteins are expressed in the kidney, liver, and gastrointestinal tract (79).

The clinical importance of the Rh30 proteins has tended to overshadow the status of the Rh50 proteins. However, *RH50* genes have a much longer evolutionary history than *RH30* and

the latter are likely to have derived by duplication from an *RH50*-like ancestor (38, 52). Indeed, while *RH50* genes are present in the genome of the basal deuterostome animals sequenced thus far, the sea urchin *Strongylocentrotus purpuratus* (echinoderms), *Ciona intestinalis* and *Ciona savignyi* (tunicates), and amphioxus (cephalochordates), *RH30* genes are absent in these species. Moreover, *RH50* and *RH30* genes are both present in teleost fish, amphibians, and mammals. Molecular evolutionary analyses have shown that in mammals Rh50 proteins evolved at a lower rate than Rh30 (38, 52), which is in line with the general trend of a higher evolutionary rate of newly duplicated genes.

Rh50 proteins share a low, albeit significant, sequence similarity (20 to 25% identity) with ammonium transport proteins of the Amt family (48, 53) although, as expected, such similarity is barely detectable for the fast-evolving Rh30 proteins. We use the term ammonium to refer to both the protonated (NH₄⁺) and the unprotonated (NH₃) forms and the term ammonia to refer specifically to NH₃.

Furthermore, expression of the human Rh50A and Rh50C (also named RhGK) can restore the growth on ammonium of a yeast mutant lacking the three endogenous *AMT* genes (49). Hence, it is now clear that Rh and Amt proteins are homologous (i.e., they are derived from a common ancestor by vertical descent), and they are assigned to the same protein family (Pfam PF00909). Molecular phylogenetic analyses (39, 72) indicated that Amt proteins can be partitioned into two clusters, named Amt- α and Amt- β (39), although the functional significance, if any, of this division remains unclear.

The biochemical function of Amt proteins as ammonium (NH₃/NH₄⁺) channels is clearly established in bacteria, fungi, and plants (74, 82), and the first evidence for the biological role of Amt in animals has recently been obtained in that ammo-

* Corresponding author. Mailing address: Institut Jacques Monod, CNRS-UMR 7592, Université Paris 6 et Paris 7, 2 Place Jussieu, 75251 Cedex 05, Paris, France. Phone: 33-1-44274185. Fax: 33-1-44275716. E-mail: giorgio.matassi@snv.jussieu.fr.

† Supplemental material for this article may be found at <http://jb.asm.org/>.

[∇] Published ahead of print on 5 October 2007.

nium channel expression is essential for brain development and function in the larva of the ascidian *Ciona intestinalis* (51). In contrast, the biochemical function of Rh50 is a subject of a controversy centered on whether the Rh50 substrate is ammonium or CO₂ (43, 82). However, it has also been suggested that Rh proteins may be relatively nonspecific channels for neutral small molecules (10).

The motivation of the present study stems from our interest in the study of the evolutionary history of the Amt/Rh protein family, which spans the entire tree of life. To date, three different evolutionary scenarios have had to be taken into account. First, bacterial and archaeal genomes code only for *AMT* genes, *RH50* genes being absent. Second, both *AMT* and *RH50* genes coexist in some genomes. This is found in a range of eukaryotes from unicellular protists, to dictyostelids, to choanoflagellates, as well as in the animal kingdom in basal taxa (cnidarians), protostomes (nematodes, insects), and deuterostomes. In the third evolutionary scenario, vertebrates possess only *RH* genes (*RH50* and *RH30*), whereas *AMT* genes are absent. Therefore, for many years, *RH* genes were considered to be specific to eukaryotes, until the genome sequence of the ammonia-oxidizing bacterium *Nitrosomonas europaea* provided the first evidence of an *RH50* gene in bacteria (13).

Ammonia-oxidizing bacteria (AOB) are obligate chemolithoautotrophs, which use NH₃ as a sole energy source and reducing power and CO₂ as the main carbon source in aerobic conditions. AOB play a central role in the biogeochemical nitrogen cycle, since they catalyze the first step in the biological oxidation of reduced forms of inorganic nitrogen: from NH₃ to nitrite (NO₂⁻). AOB achieve aerobic nitrification in two steps: first ammonia is oxidized to hydroxylamine (NH₂OH) by ammonia monooxygenase and then to NO₂⁻ by hydroxylamine oxidoreductase. However, although substantial data are available on these enzymes (5), it is not yet known how ammonium enters the cell and, in *N. europaea*, reaches intracellular concentrations as high as 1 M (62). Ammonia-oxidizing bacteria are found within both the β- and the γ-proteobacteria. Molecular phylogenies, based on 16S rRNA and ammonia monooxygenase genes, indicate that they form two monophyletic groups. Within the β-proteobacteria AOB, five clusters have been defined, among which cluster *Nitrosomonas* and *Nitrosospora* (57, 58).

In the present study, we sought to elucidate the evolutionary history of the *RH50* gene from *N. europaea* (*RH50*_{Ne}). Furthermore, given the vital role of ammonium in AOB physiology, we sought to determine whether the Rh50_{Ne} protein is involved in ammonium transport. Our phylogenetic analyses suggest that *N. europaea* acquired the *RH50* gene by horizontal gene transfer (HGT); hence, since *AMT* genes are lacking in the genome, the *RH50*_{Ne} gene may be regarded as a case of nonorthologous gene displacement (40). In addition, by functionally characterizing the Rh50_{Ne} protein and the corresponding knockout (KO) mutant, we determined that Rh50_{Ne} can mediate ammonium uptake and thus may also have replaced (displaced) Amt functionally.

MATERIALS AND METHODS

Phylogenetic analyses. The genome of *N. europaea* is available at the JGI Integrated Microbial Genomes (JGI-IMG) resource. Fifteen datasets of homologous proteins were obtained using the *N. europaea* sequences (JGI locus tags

Ne0441 to Ne0457) as a query in BLAST searches (2) against the bacterial genome sequences currently available at the JGI-IMG resource (<http://img.jgi.doe.gov/cgi-bin/pub/main.cgi>), the National Center for Biotechnology Information (NCBI) Microbial Genomes Resource (http://www.ncbi.nlm.nih.gov/sutils/genom_table.cgi), and the TIGR-CMR Comprehensive Microbial Resource (<http://cmr.tigr.org/tigrscripts/CMR/CmrHomePage.cgi>). The genome of “*Candidatus* Kuenenia stuttgartiensis” was BLAST searched at <http://www.ncbi.nlm.nih.gov/projects/genome/seq/BlastGen/BlastGen.cgi?pid=16685>.

To each data set, orthologs retrieved from the JGI-IMG (defined as bidirectional best hits from BLASTP of each genome against each other genome) were added. In order to comply with the computationally demanding maximum-likelihood approach, the sequences to be included in each data set were selected by using a distance-based phylogenetic analysis while maintaining the largest possible bacterial taxon-sampling (not shown). Sequence multiple alignments were then obtained by using either MultAlin (16) or TCOFFEE (55) and further refined by manual editing using SeaView (23). All analyses were carried out on amino acid positions, except the datasets corresponding to the Ne0442 and Ne0446 homologs (see below). Unambiguously aligned sequence blocks were extracted with Gblocks (12), whose default parameters were modified where needed to maximize the number of sites in the alignment. ProtTest 1.3 (1) was used to select the best model of protein evolution that fit the data, including the matrix of amino acid substitution, the contribution of the gamma (Γ) parameter to model the rate heterogeneity among sites and of the fraction of invariable sites (I). The substitution matrices selected were WAG (81), RtREV (19), and Blossum62 (27). In the case of the Ne0442 and Ne0446 datasets the first and second codon positions were used due to the lack of phylogenetic signal in the corresponding amino acids. Amino acid alignments were converted to nucleotide alignments by using PAL2NAL (69) and analyzed by Gblocks as described above. Two models of nucleotide sequence evolution were used HKY (26) and GTR (44). Given the model of protein and nucleotide evolution, maximum-likelihood analyses were performed by using PHYML 2.4.4 (24). Nonparametric bootstrap analysis (100 replicates, as implemented in PHYML) and an approximate likelihood ratio test (aLRT; based on a Shimodaira-Hasegawa-like procedure, <http://atgc.lirmm.fr/alrt/>) (4) were used as branch support measures.

The taxon sampling in Fig. 1A (Ne0448) included “*Acidobacteria bacterium*” (proposed name) Ellin345, *Arabidopsis thaliana*, *Archaeoglobus fulgidus*, *Aspergillus nidulans*, *Branchiostoma floridae*, *Chlamydomonas reinhardtii*, *Ciona intestinalis*, *Danio rerio*, *Dictyostelium discoideum*, *Escherichia coli*, *Homo sapiens*, “*Ca. Kuenenia stuttgartiensis*,” *Monosiga brevicollis*, *Mus musculus*, *Naegleria gruberi*, *Nematostella vectensis*, *Nitrosomonas europaea*, *Nitrosospora multifortis*, *Phytophthora ramorum*, *Phytophthora sojae*, *Saccharomyces cerevisiae*, *Strongylocentrotus purpuratus*, and *Tetrahymena thermophila*. In constructing the data set of eukaryotic homologs of NeRh50 (Ne0448), three Rh50 proteins from the protozoan infectious parasite *Trichomonas vaginalis* (TIGR-CMR) were excluded since their compositional and evolutionary rate properties deviated with respect to the data set (not shown).

Taxon sampling in Fig. 1B (Ne0445) and Fig. 1C (Ne0446) included “*Acidobacteria bacterium*” (proposed name) Ellin345, *Agrobacterium tumefaciens* C58, *Azifex aeolicus* VF5, *Anaeromyxobacter dehalogenans* 2CP-C, *Azoarcus* sp. strain EbN1, *Bdellovibrio bacteriovorus* HD100, *Blastopirellula marina* DSM 3645, *Bordetella parapertussis* 12822, *Bradyrhizobium* sp. strain BTAi1, *Brucella melitensis* biovar Abortus 2308, *Burkholderia pseudomallei* 1710b, *Campylobacter jejuni* subsp. *jejuni* NCTC 11168, *Caulobacter crescentus* CB15, *Chlorobium limicola* DSM 245, *Chromobacterium violaceum* ATCC 12472, *Colwellia psychrerythraea* 34H, *Comamonas testosteroni* KF-1 ctg65, *Deinococcus radiodurans* R1, *Escherichia coli* K-12, *Geobacter metallireducens* GS-15, *Geobacter sulfurreducens* PCA, *Geobacter uraniumreducens* Rf4, *Hahella chejuensis* KCTC 2396, *Helicobacter pylori* 26695, *Hyphomonas neptunium* ATCC 15444, *Mesorhizobium loti*, *Neisseria meningitidis* MC58, *Nitrobacter* sp. strain Nb-311A, *Nitrobacter hamburgensis* X14, *Nitrobacter winogradskyi* Nb-255, *Nitrosomonas europaea* ATCC 19718, *Nitrosomonas eutropha* C71, *Nitrosospora multiformis* ATCC 25196, *Nostoc* sp. strain PCC 7120, *Novosphingobium aromaticivorans* DSM 12444, *Oceanicola granulosa* HTCC2516, *Paracoccus denitrificans* PD1222, *Pasteurella multocida* subsp. *multocida* Pm70, *Pelobacter carbinolicus* DSM 2380, *Polaromonas* sp. strain JS666, *Pseudomonas aeruginosa* 2192, *Pseudomonas entomophila* L48, *Pseudomonas putida* KT2440, *Ralstonia eutropha* JMP134, *Ralstonia metallidurans* CH34, *Ralstonia solanacearum* GMI1000, *Rhizobium etli* CFN 42, *Rhodobacter sphaeroides* 2.4.1, *Rhodopirellula baltica* SH 1, *Rickettsia prowazekii* Madrid E, *Rubrivivax gelatinosus* PM1, *Silicibacter pomeroyi* DSS-3, “*Solibacter usitatus*” (proposed name) Ellin6076, *Sphingopyxis alaskensis* RB2256, *Stigmatella aurantiaca* DW4/3-1 gsam_11, *Synechocystis* sp. strain PCC 6803, *Thermus thermophilus* HB8, *Vibrio cholerae* O1, *Wolinella succinogenes* DSM 1740, and *Yersinia pestis* CO92.

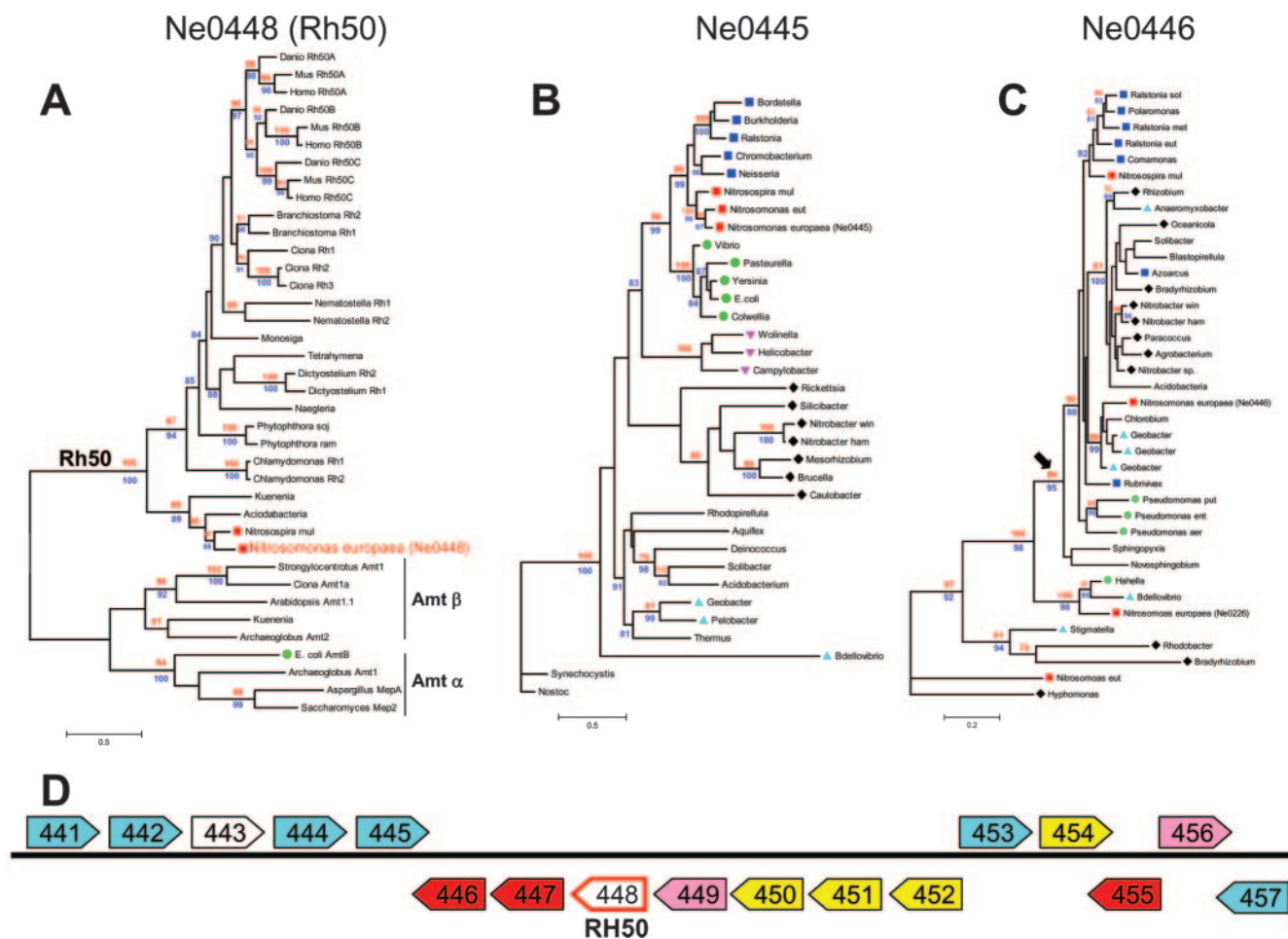


FIG. 1. Molecular phylogenetic evidence for HGT. Maximum-likelihood trees were computed by using PHYML 2.4.4 from datasets comprising 38-taxa (238 amino acid positions), 34-taxa (297 amino acid positions), and 38-taxa (316 nucleotide sites, first and second codon positions) in Ne0448 (A), Ne0445 (B), and Ne0446 (C), respectively. The evolutionary models used were RtREV+ Γ , WAG+I+ Γ , and HKY+I in Ne0448, Ne0445, and Ne0446, respectively. Support values at the nodes correspond to 100 maximum-likelihood bootstrap replicates (only values $\geq 75\%$ are shown in red) and aLRT statistics (only values $\geq 80\%$ are shown in blue). Scale bars indicate the estimated number of substitutions per site. Different symbols were used to visualize the five proteobacteria subdivisions: α , black diamonds; β , blue squares (except for nitrosomonads identified by red squares); γ , green dots; δ , cyan upward triangles; and ϵ , pink downward triangles. (A) Rh50 (Ne0448) phylogeny. The ABO *Nitrosomonas* and *Nitrospira* cluster together and with the other two bacteria “*Ca. Kuenenia*” and *Acidobacteria*. The four bacterial proteins are positioned basal to the Rh50 subtree and are distinct from the Amt subfamily. These results provide no evidence either in favor or against HGT. (B) Uroporphyrinogen III decarboxylase (Ne0445) phylogeny. An example of no HGT is that the three nitrosomonads are grouped together and cluster with the other β -proteobacteria. The β - γ proteobacteria clade is recovered as well. (C) 3-demethylubiquinone-9 3-methyltransferase (Ne0446) phylogeny. The clustering of Ne0446 with *Geobacter* (δ -proteobacteria) and *Chlorobium* (*Chlorobi*) (99% bootstrap, 99% aLRT) provides evidence of HGT. In contrast, the phylogeny of the *Nitrospira* ortholog is congruent with the species tree (clustering with the β -proteobacteria). The same topology was also obtained under the GTR model of sequence evolution (data not shown). No ortholog of Ne0446 is present in *N. eutropha*. The arrow indicates the branch leading to the subtree comprising Ne0446 orthologs. (D) Summary of the phylogenetic analyses. The *RH50*_{Ne} gene (Ne0448) and its neighbors on the chromosome are schematically represented by boxes (not to scale) that show the sense of transcription on each strand. Gene boxes are color coded as follows: cyan (no HGT), red (evidence for HGT), pink (hint for HGT), and yellow (integrases/transposase genes). The genes are Ne0441 (leucyl aminopeptidase, cluster of orthologous groups [COG], COG0260), Ne0442 (DNA polymerase III chi subunit, COG2927), Ne0443 (hypothetical protein; could not be analyzed; see Results), Ne0444 (valyl-tRNA synthetase, COG0525), Ne0445 (uroporphyrinogen III decarboxylase, COG0407), Ne0446 (hypothetical protein homologous to the 3-demethylubiquinone-9 3-methyltransferase, Pfam PF06983), Ne0447 (hypothetical protein homologous to 3-methyladenine DNA glycosylase I, COG2818), Ne0448 (Rh50, INTERPRO IPR010256), Ne0449 (aspartate/glutamate racemase, COG0796), Ne0450 (integron integrase IntI, PF00589, IPR11946, COG582), Ne0451 (integrase catalytic core, PF00665, IPR001584), Ne0452 (transposase IS911, IPR002514), Ne0453 (patatin-like phospholipase, PF01734), Ne0454 (integrase catalytic core, PF00589), Ne0455 (prokaryotic DksA/TrA R C4-type zinc finger, PF01258), Ne0456 (esterase/lipase/thioesterase, COG0596), and Ne0457 (hypothetical protein, COG5316).

Strains, plasmids and, *N. europaea* culture conditions. The strains and plasmids used in the present study are described in Table 1. *N. europaea* cells were grown in liquid medium (29) containing 25 mM $(\text{NH}_4)_2\text{SO}_4$ in the dark at 30°C on a rotary shaker (200 rpm) and reached an optical density at 600 nm (OD_{600}) of 0.1 in approximately 3 to 4 days. For growth of *N. europaea* on solid medium,

the liquid medium was modified by adding 1% agar R2A (Difco Laboratories, Detroit, MI) and by replacing the phosphate buffer with 50 mM *N*-tris(hydroxymethyl)methyl-2-aminoethane sulfonic acid buffer (pH 7.8) (28). *N. europaea* cells were streaked onto an autoclaved Nytran membrane (Schleicher & Schuell), which was laid out on solid medium and then incubated at 30°C; the membrane

TABLE 1. Strains and plasmids

Strain or plasmid	Description ^a	Source or reference
Strains		
<i>E. coli</i> GT1000	<i>rbs lacZ::IS gyrA hutC_K ΔglnK-amtB</i>	17
<i>S. cerevisiae</i> 23344c	<i>MATα ura3</i>	50
31019b	<i>MATα ura3 mep1Δ mep2Δ::LEU2 mep3Δ::Km MX2</i>	50
<i>N. europaea</i> ATCC 19178	Wild type	ATCC ^b
<i>RH50_{Ne}</i> -KO	<i>RH50::Km</i> insertion mutant	This study
Plasmids		
pAD7	<i>RH50</i> -His ₆ cloned into pESV2	This study
pAD8	<i>RH50</i> cloned into pESV2	This study
pAD9	<i>RH50</i> -His ₆ cloned into pDR195	This study
pAD10	<i>RH50</i> cloned into pDR195	This study
pDR195	Yeast expression vector (<i>URA3</i> ; <i>Amp^r</i>)	59
pESV2	<i>amtB8</i> (<i>ΔglnK</i> derivative of pESV1)	30
pJT6E	<i>glnK-amtB15</i> wild-type <i>AmtB_{Ec}</i>	31
pTF14	Wild-type <i>AmtB_{Ec}</i> into pDR195	Tim Fulford
pCR2.1-TOPO	Cloning vector (<i>lacZα Km^r/Amp^r fl ori</i>)	Invitrogen
pQBIfN1	Expression vector (<i>GFP Amp^r pUC ori</i>)	Q-Biogen
pRL448	pRL139 derivative (<i>Amp^r Km^r</i>)	21
pKD13	Template plasmid (<i>oriRγ Km^r</i>)	18
pNe1	<i>RH50_{Ne}</i> cloned into pCR2.1-TOPO	This study
pNe2	<i>RH50_{Ne}</i> cloned into pQBIfN1	This study
pNe3	pNe2 <i>RH50::Km</i>	This study
pNe4	pRL448 <i>RH50::Km</i>	This study

^a Amp^r, ampicillin resistance; Km^r, kanamycin resistance.

^b ATCC, American Type Culture Collection.

was transferred to new medium every 4 days. Cell suspensions were grown in the dark at 30°C under constant stirring (800 rpm). In all experiments, kanamycin was used at a concentration of 10 μg ml⁻¹.

Cloning of the *RH50_{Ne}* gene. Genomic DNA was prepared from 10 ml of a 4-day culture of *N. europaea* (OD₆₀₀ = 0.1) by using a Wizard genomic preparation kit (Promega). The *RH50* gene was amplified by PCR using the DyNAzyme EXT DNA polymerase (Finnzymes) between primers P1 and P2 (see Table S1 in the supplemental material and for all other primers). A standard PCR protocol was used with an annealing temperature of 60°C and a final extension of 7 min at 72°C. The PCR product was inserted into pCR2.1-TOPO (pNe1; Table 1) by using a TOPO TA cloning kit (Invitrogen/Life Technologies) and sequenced.

Construction of Rh50 expression vectors. Plasmids pAD7 and pAD9 code for Rh50_{Ne} with a His₆ tag at the C terminus, and plasmids pAD8 and pAD10 encode the wild-type Rh50_{Ne} protein. Plasmids pAD7 and pAD8 were designed for heterologous expression in *E. coli*, and pAD9 and pAD10 were designed for expression in *S. cerevisiae*. To construct pAD7 and pAD9, the coding sequence of *RH50_{Ne}* was amplified from pNe1 using the primers AD1 and AD2. For pAD8 and pAD10 constructs, pNE1 was amplified with AD3 replacing AD2. The PCR products were inserted into the XhoI and BamHI sites of pDR195 (pAD9, pAD10) and into the NdeI and BamHI sites of pESV2 (pAD7, pAD8).

Construction of the recombinant plasmid for insertional mutagenesis. *RH50_{Ne}* was amplified by PCR from genomic DNA using primers P1 and P2. The amplified product was then digested with SacII and EcoRI and inserted into the corresponding cloning sites of pQBI25fN1 (pNe2). The kanamycin cassette was

amplified from the pKD13 plasmid by using primers Km1 and Km2 and inserted into pNe2 between nucleotide positions 628 and 696 of the *RH50* gene (nucleotide 1 is the A of the start codon ATG), creating plasmid pNe3. For the mutagenesis experiment, the *RH50::Km* fragment was PCR amplified from pNe3 using P2 and P3 primers and inserted into the EcoRI site of pRL448 (kindly provided by Norman Hommes). The final construct, pNe4, was confirmed by sequencing.

Insertional mutagenesis of *RH50_{Ne}*. *N. europaea* cells were inoculated in 500 ml of medium and allowed to reach an OD₆₀₀ of 0.1. Cells were harvested and washed three times with sterile H₂O and taken up in 1 ml of sterile H₂O. Electroporation was performed as described previously (28). Briefly, cell suspension (120 μl) and DNA (1 μl of 1-μg μg⁻¹ solution) were mixed in a 1-mm-gap electroporation cuvette and pulsed at 1,200 V and 25 μF, with resistance set to infinite. After electroporation, cells were immediately transferred into 500 ml of liquid medium and grown for 16 h at 30°C in the dark before kanamycin was added at a final concentration of 10 μg ml⁻¹. Several kanamycin-resistant clones were isolated on solid medium. The disruption of the *RH50_{Ne}* gene on the chromosome was confirmed by PCR amplification by using primer pairs localized in the kanamycin cassette and the *RH50_{Ne}* flanking region (Km1-P5 and Km2-P4) and in the 5' and 3' flanking regions of the *RH50_{Ne}* gene (P7-P8) that was also sequenced. As a negative control, PCR was performed between primers P6 (located in the deleted region of the *RH50_{Ne}* gene) and P7 (5' flanking region).

Growth rate of *N. europaea* wild type and *RH50* KO mutant. Biomass was produced in a chemostat from which cells (~8 × 10⁸ cells ml⁻¹) were inoculated in mineral medium (63) and grown in the dark at 30°C. The experiments were performed in 300-ml Erlenmeyer flask containing 75 ml of mineral medium at different concentrations of ammonium (1.0, 2.0, and 10 mM ammonium chloride, pH 7.4; n = 4). At regular time intervals samples were taken, and the ammonium, nitrite, and protein concentrations were measured as previously described (9, 63, 73). We define lag phase as the time required at 10 mM NH₄⁺ in the medium to oxidize the first 200 μM, at 2 mM NH₄⁺ the first 200 μM, and at 1 mM NH₄⁺ the first 100 μM.

Western blotting. Yeast membranes were prepared as described elsewhere (www.stke.org/cgi/content/full/sigtrans/2005/275/pl3). Yeast cells were grown in 50 ml of yeast nutrient broth (YNB) plus 0.2% glucose (wt/vol) at 30°C to an OD₆₀₀ of 1.0 and then harvested by centrifugation at 700 × g for 5 min at 4°C. The cell pellet was resuspended in 1 ml of 50 mM Tris-HCl (pH 7.5) supplemented with a mixture of protease inhibitors (Roche). The cells were transferred into a 2-ml tube, and 300 μl of chilled glass beads (size range, 425 to 600 μm; Sigma) was added. The cells were lysed by vigorous vortex mixing seven times for 30 s and then separated by treatment at 1 min on ice. The lysate was centrifuged at 700 × g for 20 min at 4°C. The supernatant was spun at 700 × g for 10 min at 4°C. The membrane and cytosolic fractions were separated by a centrifugation step at 150,000 × g for 2 h at 4°C. The cytosolic fraction was kept for analysis, and the membrane pellet was resuspended in 50 mM Tris-HCl (pH 7.5) with 1% Triton as described above. The resulting supernatant (membrane) was kept for Western blot analysis. Western blotting was performed as previously described (17), and proteins were detected with anti-His antibodies (QIAGEN) or anti-AmtB antibodies.

***E. coli* transport assays (unwashed).** *E. coli* strains were grown in Luria medium. For growth in nitrogen-limiting conditions, a modified M9 medium was used (M9Gln) that contained 0.2% glucose as a carbon source and glutamine (which replaced ammonium) at 200 μg ml⁻¹. The unwashed assays were performed with Rh50_{Ne}-expressing cells (GT1000 cells transformed with pAD7 or pAD8) and *E. coli* AmtB-expressing cells (GT1000 transformed by pJT6E vector). Experiments were carried out at room temperature as described previously (32).

***S. cerevisiae* transport assays (washed).** [¹⁴C]methylammonium ([¹⁴C]MA) uptake assays (adapted from a previously reported method [80]) were performed with cells expressing Rh50_{Ne} (31019b cells transformed with pAD9 or pAD10), *E. coli* AmtB cells (31019b transformed with pTF14), and control cells (23344c and 31019b cells transformed with empty vector pDR195). Cells were grown overnight in YNB minimal medium (Difco Laboratories) supplemented with 3% (wt/vol) glucose and 0.2% (wt/vol) glutamate. When the cells exceeded an OD₆₀₀ of 0.5, they were washed and resuspended in 3% (wt/vol) glucose buffered with 10 mM phosphate (pH 6.0 or 7.0) or 50 mM HEPES (pH 8.0). In the assay, a final concentration of 500 μM MA was used. Briefly, 500 μl of 5 mM MA containing 0.725 μCi of [¹⁴C]MA (Amersham Biosciences) was added to 4.5 ml of the culture. Uptake was measured by removing 500-μl aliquots at different time intervals; the sample was then immediately applied onto a prewashed 0.45-μm-pore-size filter (Millipore) placed on a suction system. The filters were immediately washed with 5 ml of a washing buffer (10 mM phosphate buffer [pH 6.0],

500 μ M MA), and radioactivity was measured by scintillation counting. The assay was performed at room temperature.

Restoration of growth phenotype in *S. cerevisiae*. The *S. cerevisiae* wild-type (23344c) and ammonium transporter-deficient (31019b; Δ *nep1-3*) strains were transformed with the *RH50_{Ne}* gene carried on pAD9 or pAD10. Both yeast strains were plated onto YNB (1.7 g liter⁻¹) supplemented with 3% (wt/vol) glucose as a carbon source and solidified with 0.8% agarose. The nitrogen sources used were glutamate 0.2% (wt/vol) and ammonium chloride at 0.5, 1, and 3 mM. The medium was adjusted to pH 6.0, 6.5, or 7.0 with 10 mM phosphate buffer.

[¹⁴C]MA uptake assay in *N. europaea*. *N. europaea* cells were harvested from a chemostat culture (after five volume changes) and were washed twice in mineral medium (63) without ammonium. Details on growth conditions in the chemostat are given in the supplemental material. The cell number was adjusted to about 5×10^9 cells ml⁻¹. The bacterial suspensions (28°C) were stirred (800 rpm), and the experiments were started by adding MA or ammonium. [¹⁴C]MA (Biotrend, Köln, Germany) at 55 mCi/mmol was used as radiotracer. The assays were designed as previously described (72, 80) and were performed as unwashed assays. As a control experiment, the buffer containing [¹⁴C]MA was passed over a polycarbonate filter (0.2- μ m pore size), the radioactivity of the filter was measured, and the unspecific binding of [¹⁴C]MA for inactivated (heat-treated) *N. europaea* cells was evaluated and used as a baseline. Radioactivity was measured by liquid scintillation counting (BETAmatic BASIC counter; Kontron Analytical, Münchenstein, Switzerland).

RESULTS

Evidence for HGT of *RH50_{Ne}*. We have BLAST searched about 700 bacterial and 34 archaeal completed and draft genome sequences for *RH50* homologs, and we identified *RH50*-like sequences in four bacterial species: two β -proteobacterial AOB, *N. europaea* ATCC 19718 (*Nitrosomonas* cluster; JGI-IMG locus tag Ne0448/NCBI Entrez protein accession no. NP_840535), and *Nitrosospora multiformis* ATCC 25196 (*Nitrosospora* cluster; locus tag Nmul_A0516/YP_411216), the acidobacterium *Acidobacteria bacterium* Ellin345 (locus tag Acid345_3596/YP_592671), and the planctomycete “*Ca. Kuenenia stuttgartiensis*” (CAJ711226). The existence of *RH50* genes in the two AOB was reported previously (13, 43). In addition, we noted that *AMT* genes are missing in the two AOB genomes, whereas *Acidobacteria bacterium* and “*Ca. Kuenenia*” possess two (Acid345_3596/YP_593520 and Acid345_3596/YP_590566) and four (CAJ71754, CAJ71757, CAJ71760, and CAJ74453) *AMT* genes, respectively.

The *RH50* gene was found to be missing in the genomes of other members of the corresponding clades. Based on BLAST searches against the currently available genome sequences (JGI-IMG), two other AOB, *N. eutropha* C71 (β -proteobacteria, *Nitrosomonas* cluster) and *Nitrosococcus oceani* ATCC 19707 (γ -proteobacteria), appeared to lack both *RH50* and *AMT* genes. “*Ca. Kuenenia stuttgartiensis*” belongs to the phylum *Planctomycetes*, and BLAST searches we have carried out against the two other genomes currently available in this phylum (JGI-IMG), namely, *Rhodopirellula baltica* SH1 (complete) and *Blastopirellula marina* DSM 3645 (draft), indicate that they lack *RH50* genes while possessing three and four *AMT* genes, respectively. Together with “*Acidobacteria bacterium*,” two other genome sequences are currently available in the phylum *Acidobacteria*: *Solibacter usitatus* Ellin6076 (JGI-IMG) and “*Acidobacteria capsulatum*” (proposed name) ATCC 51196 (TIGR). Again, BLAST searches revealed the lack of *RH50* and the presence of at least two *AMT* genes in *A. capsulatum* and *S. usitatus*. Interestingly, the genomes of *A. bacterium* and “*Ca. Kuenenia stuttgartiensis*” also possess two

and four copies of the *AMT* gene, respectively. To our knowledge, this is the first case described thus far of coexistence of *AMT* and *RH50* genes in bacterial genomes.

The presence of *RH50* genes in only four bacterial species could be accounted for by a large number of independent gene losses in all of the bacterial lineages known to date. However, this scenario is classically regarded as highly unlikely. The alternative and most parsimonious explanation is that the bacterial *RH50* genes have been acquired by HGT (also described as lateral gene transfer), an evolutionary process whereby genetic material is exchanged between distantly related species (20, 41, 56). Provided enough taxon sampling is available, phylogenetic analysis remains the most powerful method to detect the likely occurrence of an HGT event (41, 70). Briefly, a known phylogenetic species tree, taken as a reference, is compared to the tree inferred from the gene under study and incongruent topologies are regarded as evidence of HGT. However, it has been stressed that any kind of evidence of HGT is “always a probabilistic one and rarely direct” (41).

To explore the HGT hypothesis for *NeRH50*, we carried out phylogenetic analyses on a data set comprising a subset of 29 *Rh50* protein sequences, as well as four *Amt- α* and five *Amt- β* proteins, using a maximum-likelihood approach. The data set was arbitrarily chosen in order to render the analyses computationally tractable while including the largest possible taxon sampling for eukaryotic *Rh50* proteins. Our results show that the *Rh50* proteins from *N. europaea* and *N. multiformis* are closely related, as expected (87% bootstrap, 88% aLRT support; see Materials and Methods) and that, together with their homologs from *A. bacterium* and “*Ca. Kuenenia stuttgartiensis*,” they are distinct (100% bootstrap, 100% aLRT) from the *Amt* subfamily (Fig. 1A).

The four bacterial *Rh50* proteins were clearly separated from the eukaryotic homologs and are positioned at the base of the *Rh50* subfamily clade. Therefore, in this case no comparison between species tree and gene tree can be done, and thus phylogenetic evidence for *RH50_{Ne}* HGT cannot be obtained, since the basal positioning of the bacterial *Rh50* proteins is to be expected, whether they are “true” bacterial or “HGT-acquired” sequences that have accumulated enough divergence. Consequently, we sought evidence of HGT by analyzing the 16 genes (Fig. 1D) that are neighbors of *RH50* (Ne0448) on the *N. europaea* chromosome (locus tags Ne0441 to Ne0457).

No phylogenetic analysis could be carried out in the case of Ne0443 (that encodes a hypothetical protein) since no hits were found by BLAST search, except for one sequence in *N. eutropha* (locus tag Neut_0601). For each of the remaining 15 genes we carried out phylogenetic analyses in order to detect incongruence between the species tree, the proteobacterial tree in this case, and the gene tree. The current phylogeny of the five subdivisions of proteobacteria (based on 16S and 23S rRNA, whole-genome comparisons, and molecular signatures) give δ and ϵ subdivisions as early branching (which one of them is more basal is not clear) and largely support the (α (β , γ)) topology (25, 71).

Figure 1B shows an example of congruence between species tree and gene tree (i.e., no HGT) in the case of the uroporphyrinogen decarboxylase. The three orthologs from the AOB *N. europaea* (Ne0445), *Nitrosomonas eutropha*, and *N. multiformis* cluster together (Fig. 1B, red squares) and are confi-

dently (99% bootstrap, 99% aLRT) located within the β -proteobacteria (Fig. 1B, blue squares). In contrast, the phylogeny of the 3-demethylubiquinone-9 3-methyltransferase gene (Fig. 1C) shows on the one hand the incongruent clustering of Ne0446 with *Geobacter* spp. (δ -proteobacteria) and with *Chlorobium limicola* (*Chlorobi*) (99% bootstrap, 99% aLRT) and on the other hand the congruent clustering of the *Nitrosospira* ortholog (no ortholog present in *N. europaea*) with the β -proteobacteria. These results suggest that Ne0446 entered the *N. europaea* genome via an HGT event. Incidentally, the *Chlorobium* gene seems to have undergone HGT as well, for we have BLAST searched eight *Chlorobi* genomes (*Bacteroides fragilis*, *B. thetaiotaomicron*, "*Chlorobium chlorochromatii*" (proposed name), "*C. ferrooxidans*" (proposed name), *C. phaeobacteroides*, *C. tepidum*, and *Porphyromonas gingivalis*) and could not find homologs. To infer this phylogeny, we have used the first and second codon positions of the genes, since the analysis based on amino acids did not provide sufficient resolution (not shown). The results of the phylogenetic analyses of the other 13 neighboring genes are given in the supplemental material (all datasets and multiple alignments are available upon request).

Supporting evidence for the HGT hypothesis is given by the presence of three genes adjacent to and upstream from the *RH50* (Ne0448) gene on the same strand, which code for an integron-integrase *intI* (Ne0450, INTERPRO IPR11946), a catalytic-core integrase (Ne0451, IPR001584; another such integrase is coded by Ne0454 on the other strand), and an *IS911* transposase (Ne0452), all proteins being involved in processes of DNA recombination and exchange. We carried out phylogenetic analyses of these four proteins, and we detected evidence of HGT in the case of Ne0454, which clusters with α -proteobacteria, but no evidence of HGT for Ne0450, Ne0451, and Ne0452 (see Fig. S3 in the supplemental material).

Three additional neighboring genes are likely HGT candidates, although with various levels of confidence. Significant evidence was obtained for Ne0447: no homologs were found in nitrosomonads other than *N. europaea*, and BLAST searches identified homologs only in α - and γ -proteobacteria, with which Ne0447 clusters (see Fig. S2 in the supplemental material). In the case of the prokaryotic DksA/TraR transcriptional regulator, Ne0455, *N. multififormis* and *N. europaea* orthologs clustered with the γ -proteobacteria, while the β -proteobacterial homologs clustered with the α -proteobacteria (see Fig. S4 in the supplemental material). In the phylogeny of the aspartate-glutamate racemase, Ne0449 and its *N. europaea* ortholog cluster with two γ -proteobacteria and a δ -proteobacterium (92% aLRT, but no bootstrap support), thereby suggesting the occurrence of an HGT event (see Fig. S2 in the supplemental material). Evidence that may indicate HGT was also obtained for the Ne0456 gene, which is separated by the α - and β -proteobacterial orthologs (81% aLRT, but no bootstrap support) (see Fig. S4 in the supplemental material). Finally, we obtained no evidence for HGT in the case of Ne0441, Ne0442, Ne0444, Ne0453, and Ne0457 (see Fig. S1, S2, and S4 in the supplemental material).

The results of the analyses on the 16 gene neighbors of *RH50_{Ne}* (Ne0448), located in the chromosomal region spanning about 20 kb of the *N. europaea* chromosome, are sche-

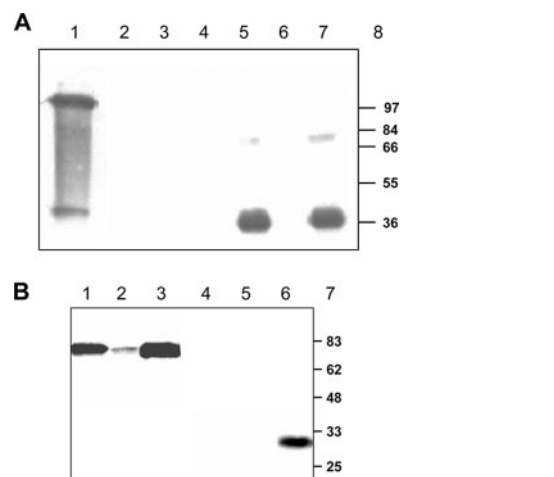


FIG. 2. Expression of Rh50_{Ne} in *E. coli* and *S. cerevisiae*. (A) Detection and localization of Rh50_{Ne} when expressed in *E. coli*. A Western blot was performed with anti-His antibody. Lane 1, purified *E. coli* AmtB-His₆; lanes 2 to 4, GT1000(pAD8) expressing NeRh50; lanes 5 to 7, GT1000(pAD9) expressing Rh50_{Ne}-His₆; lanes 2 and 5, whole-cell extract; lanes 3 and 6, cytoplasmic fraction; lanes 4 and 7, membrane fraction; lane 8, molecular mass markers (indicated in kilodaltons). (B) Detection and localization of Rh50_{Ne} when expressed in *S. cerevisiae*. Lanes 1 to 3, *S. cerevisiae* strain 31019b(pTF14) expressing *E. coli* AmtB detected using anti-AmtB antibody; lanes 4 to 6, *S. cerevisiae* strain 31019b(pAD9) expressing Rh50_{Ne} detected using anti-His antibody; lanes 1 and 4, whole-cell extract; lanes 2 and 5, cytoplasmic fraction; lanes 3 and 6, membrane fraction. All lanes were loaded with 5 μ g of protein, and consequently the relative concentrations of membrane proteins are greater in the membrane fraction than in the whole-cell extract. Lane 8, molecular mass markers (indicated in kilodaltons).

matically summarized in Fig. 1D. Overall, our results suggest that there are two regions that are candidates for HGT. The first one consists of the Ne0455 gene and possibly of Ne0456; adjacent to this region is Ne0454, which codes for an integrase. The second region comprises at least Ne0446, Ne0447, and Ne0449. We deduce by inference that Ne0448 (*RH50_{Ne}*), which is embedded in this region, is likely to have undergone HGT.

Functional characterization of *RH50_{Ne}*. Given that there are no *AMT* genes in the *N. europaea* genome, we sought to determine whether the *RH50* gene could have functionally replaced *AMT*. To test this hypothesis, we used two strategies. First, we cloned *RH50_{Ne}* in suitable vectors and expressed it in *E. coli* and *S. cerevisiae* deletion mutants deficient in ammonium uptake. Second, we constructed a knockout *RH50_{Ne}* (*RH50_{Ne}*-KO) mutant and compared its growth on ammonium and its ability to transport MA to that of the wild type.

Plasmid constructs were made that encoded both the wild-type *Ne*Rh50 protein and a derivative His-tagged (His₆) at the C terminus. The latter construct facilitated detection of the protein by Western blotting with an anti-His₆ antibody. These constructs were used to express Rh50_{Ne} in the ammonia channel mutant strains *E. coli* GT1000 (Δ *amtB*) and *S. cerevisiae* strain 31019b (Δ *mep1-3*). NeRh50 was correctly localized to the membrane both in *E. coli* (Fig. 2A, lanes 5 to 7) and in yeast (Fig. 2B, lane 6), as determined by Western blot analysis of cell fractions. In the case of yeast in particular the Rh50_{Ne} signal was much stronger in the membrane fraction than in the whole-cell extract, but the material loaded in Fig. 2B, lane 6, is

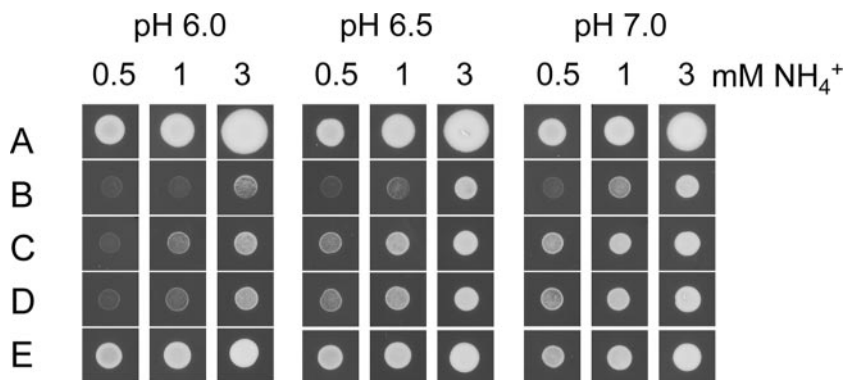


FIG. 3. *RH50_{Ne}* restores growth in the *S. cerevisiae* $\Delta mep1-3$ mutant. Growth was determined after 5 days at 30°C on minimal YNB medium containing ammonium chloride at 0.5, 1.0, or 3.0 mM. Experiments were carried out with media adjusted to pH 6.0, 6.5, or 7.0. The strains tested were 23344c(pDR195) (*mep*⁺) (A), 31019b(pDR195) ($\Delta mep1-3$) (B), 31019b(pAD10) (Rh50_{Ne}) (C), 31019b(pAD9) (Rh50_{Ne}-His₆) (D), and 31019b(pTF14) (AmtB_{Ec}) (E).

concentrated relative to that in lane 4. The apparent molecular mass of the predominant molecular species of Rh50_{Ne} was ~36 kDa in *E. coli* and ~30 kDa in yeast. This could predictably correspond to a folded form of the monomer, which has a theoretical molecular mass of ~43 kDa. A small percentage of the Rh50_{Ne} expressed in *E. coli* ran as a higher-molecular-mass species that could reflect a trimeric form.

We assessed the transport activity of Rh50_{Ne} with or without the His tag by measuring the influx the ammonium analogue [¹⁴C]MA at different pH values in *E. coli* and yeast cells using washed and unwashed assays, respectively. The washed assay measures MA influx into cells and its subsequent assimilation into methylglutamine by glutamine synthetase (32), whereas the unwashed assay measures all MA influx into the cell, including that which is not converted to methylglutamine. No significant transport activity was detected in *E. coli* cells either at 20 μ M MA (pH 7.0) or at 250 μ M (pH 7.0 and 8.0) (data not shown). Similarly, no significant accumulation of [¹⁴C]MA was observed in yeast cells grown at 500 μ M MA at pH 6.0, 7.0, or 8.0 (data not shown). Therefore, we used an alternative approach to assess Rh50_{Ne} ammonium channel activity by analyzing whether the expression of the protein (with or without a His tag) could restore the ammonium-dependent growth phenotype of the *S. cerevisiae* 31019b strain, and we compared it with the corresponding activity of the *E. coli* AmtB protein (AmtB_{Ec}) expressed in the same strain.

The transformed yeast cells were plated on nitrogen-free medium supplemented with 0.5, 1.0, or 3.0 mM ammonium chloride at three different pH values (6.0, 6.5, and 7.0). After 5 days of incubation at 30°C, Rh50_{Ne} expression restored the growth of the yeast mutant in a pH-dependent manner (Fig. 3). At pH 6.0 growth restoration was only apparent on 1 mM ammonium chloride, but when the pH was raised to 6.5 or 7.0 the restoration of growth was apparent on 0.5 mM ammonium and was significantly improved at 1 mM ammonium. Rh50_{Ne} activity was identical with or without His tag. The phenotype observed for Rh50_{Ne} was different from that obtained with AmtB_{Ec}, since expression of the latter restored growth at all pHs and at all of the ammonium chloride concentrations tested (Fig. 3E).

We also studied the ammonium transport properties of

Rh50_{Ne} in *N. europaea*. To this end, we inactivated the *RH50_{Ne}* gene by insertional mutagenesis using a kanamycin resistance cassette. In a first set of experiments we compared the growth of *N. europaea* wild-type and *RH50_{Ne}*-KO strains at different concentrations of ammonium (1.0, 2.0, and 10 mM ammonium chloride, pH 7.4; *n* = 4). Growth was monitored by measuring ammonia oxidation and nitrite formation. At low ammonium concentrations the lag phase of the KO mutant was significantly longer than that of the wild type (115 \pm 8 min versus 85 \pm 5 min at 1 mM and 85 \pm 6 min versus 71 \pm 2 min at 2 mM, respectively). We also compared the growth of the wild type and the KO mutant at various concentrations of CO₂ (0.04, 0.1, 0.5, and 1.0%) in a chemostat culture, and we did not detect any effect on the growth rate, growth yield, or ammonia oxidation activity (data not shown).

Finally, we compared MA influx in *N. europaea* wild-type and *RH50_{Ne}*-KO strains by performing unwashed transport assays, again using [¹⁴C]MA as a radiotracer. The MA uptake activities were examined during the first 4 min, and the results (Fig. 4) demonstrate that the MA uptake rate of the mutant cells (58.6 \pm 18.2 nmol mg of protein⁻¹ min⁻¹) was about five times lower than of wild-type cells (252.7 \pm 78.9 nmol mg protein⁻¹ min⁻¹). From these data, we conclude that the Rh50 protein is involved in ammonium uptake in *N. europaea*.

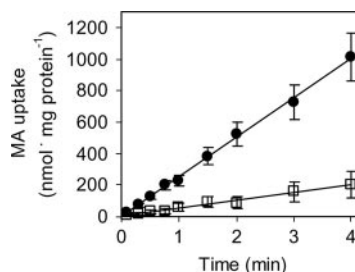


FIG. 4. [¹⁴C]MA uptake in *N. europaea* wild type and *RH50* KO mutant. The MA concentration in the uptake assay was adjusted to 10 mM, and the cell number was 5×10^9 cells ml⁻¹. The results are means \pm the standard deviation (*n* = 6). Symbols: ●, *N. europaea* wild type; □, *RH50_{Ne}*-KO mutant.

DISCUSSION

HGT of *RH50* to *N. europaea*. Not only does evolution at the molecular level proceed via the inheritance of genetic material by vertical descent from a common ancestor, but organisms can also inherit genetic information by nonvertical descent due to the ability of DNA to be carried across species by bacteriophages and plasmids, to be exchanged by transformation, and to be absorbed from the environment and integrated in the genome. These “alternative” processes are collectively referred to as horizontal (or lateral) gene transfer, which is now recognized as a major force in the evolution of at least prokaryotic genomes (20, 41, 56).

We used a phylogenetic approach to assess the likelihood of HGT of the *RH50* gene in *N. europaea*. This analysis was not very informative since, together with the other three bacterial Rh50 proteins, Rh50_{Ne} occupies a basal position within the Rh50 clade (Fig. 1A). Therefore, we could not determine whether the genes encoding these four proteins are “truly” bacterial or “HGT-acquired” sequences that have accumulated divergence. Similar basal positioning was reported for the *Prostheco bacter* *BtubA* and *BtubB* tubulin HGT candidate genes (34). However, we have gathered four kinds of indirect evidence supporting the HGT of *RH50*_{Ne}, which may also hint at HGT as being responsible for the spread of the *RH50* gene to *N. multiformis*, “*Ca. Kuenenia stuttgartiensis*,” and *A. bacterium*.

First, only four species out of more than 700 bacterial genomes possess a copy of an *RH50* gene. Second, the *RH50* gene is missing in the sequenced genomes of two AOB (*N. eutropha*, and *N. oceani*), two planctomycetes (*R. baltica* and *B. marina*), and two acidobacteria (*A. capsulatum* and *S. usitatus*). Third, and most importantly, we have shown that *RH50*_{Ne} (Ne0448) is embedded in a region comprising three genes (Ne0446, Ne0447, and Ne0449), all of which, according to our phylogenetic analyses, are candidate horizontally transferred genes (Fig. 1D). Fourth, this HGT candidate region is adjacent to three genes coding for an integron integrase *IntI* (Ne0450), a catalytic-core integrase (Ne0451), and an *IS911* transposase (Ne0452) (Fig. 1D). In particular, integron *intI* genes are involved in the formation of integron cassettes which are believed to “function as a general gene-capture system in bacterial adaptation” and thus are regarded as key players in HGT events (60). Moreover, the second copy of the *IntI* integrase gene in the *N. europaea* genome (Ne2189) was shown to be able to promote excision and integration of resistance gene cassettes (46). The region spanning Ne0446 to Ne0450 may thus correspond to an integron cassette, and we infer that the *N. europaea RH50* gene entered the genome via HGT.

HGT of *RH50*_{Ne}: hypothetical scenarios. Two scenarios can be envisaged to account for the presence of the *RH50* gene in *N. europaea* (and possibly in *N. multiformis*). We may assume that a single HGT event has occurred in the common ancestor to the AOB β -proteobacteria. If such were the case, we ought to deduce that, for some as-yet-unexplained reasons, a gene loss event has occurred specifically in the *N. eutropha* lineage (the same AOB cluster as *N. europaea*). Alternatively, a single HGT event may have occurred in the *N. europaea* lineage. The first scenario would be favored if we were to demonstrate that the *N. multiformis RH50* gene has also been acquired by HGT.

Phylogenetic analyses are currently under way to test the hypothesis of HGT for the *RH50* genes from *Nitrosospira multiformis*, “*Ca. Kuenenia stuttgartiensis*,” and *Acidobacteria bacterium* and will be presented elsewhere.

The phylogeny of the bacterial Rh50 proteins (Fig. 1A) contains interesting and puzzling information nonetheless. We note that the branches separating the AOB (*N. europaea* and *N. multiformis*) from *Acidobacteria* sp. and “*Ca. Kuenenia*” are much shorter than expected given that those species belong to three different phyla. In trying to understand the evolution of the bacterial *RH50* genes, we reason as if three independent HGT events had occurred in the three lineages leading to AOB β -proteobacteria, “*Ca. Kuenenia*,” and *Acidobacteria*. Short branches may result from exceptionally slow evolution rates (be it adaptive or due to regional or genome-wide mutational biases) of the four *RH50* genes, which is highly unlikely (even more so if these genes were “truly” bacterial). Alternatively and most likely, these short branches may indicate recent HGT events. However, such an explanation contrasts with the clear separation between the bacterial *RH50* genes and their eukaryotic homologs. To account for this apparent incongruence, we propose a working hypothesis whereby the donor *RH50*, likely of eukaryotic origin, may have first entered an “intermediate” prokaryote and then may have been transferred to the three lineages analyzed here. However, the currently available taxon sampling for bacterial *RH50* genes, which is expected to expand as more genome data become available, does not allow us to draw any conclusion in this respect. Overall, taking also into account the potential role of the *IntI* integrase in the spread of *RH50*, we envisage a eukaryote–prokaryote–prokaryote HGT scenario as a possibility, even though this phenomenon has not been described in the literature thus far.

To date, the vast majority of the reported cases of the transfer of genetic material among the three domains of life concern reciprocal exchanges from bacteria to archaea and from prokaryotes to eukaryotes (20, 41). In contrast, evidence for DNA transfer from eukaryotes to prokaryotes is much rarer and is mainly restricted to symbiotic or parasitic relationships (41). Following the hypothesis of a eukaryotic origin for the *RH50* gene in *N. europaea*, this HGT event may be one of the rare cases of eukaryotic versus bacterial transfer.

HGT of *RH50*_{Ne}: a case of nonorthologous gene displacement. Koonin et al. proposed to classify HGT events into a minimum of three categories “with respect to the relationships between the horizontally acquired gene and homologous genes (if any) preexisting in the recipient lineage” (41). In one category, a phylogenetically “distant” ortholog is acquired by HGT, followed by xenologous gene displacement (xeno = foreign), i.e., the elimination of the preexisting gene. In the other two categories, HGT drives the acquisition of either an unrelated gene, which is absent in other members of the same clade, or a distantly related paralog. Again, the acquisition of the new gene may result in the loss of the resident gene; in such a case the phenomenon is dubbed nonorthologous gene displacement (40).

The presence of a copy of the *RH50* gene in only four bacterial species out of the more than 700 prokaryotic genomes (bacteria and archaea) we have analyzed, among which AMTs are widely distributed, suggests that *RH50* is likely to have arisen by a gene duplication event from an *AMT*-like

eukaryotic ancestor. The acquisition of *RH50* by *N. europaea* may be included in the HGT category of xenologous gene displacement (41), if we follow the most recent definition of this phenomenon given by Koonin (42) and consider *AMT* and *RH50* as members of the same orthologous cluster (COG0004). However, if we consider *AMT* and *RH50* as paralogs, then the HGT of *RH50*_{Ne} is to be regarded as a non-orthologous gene displacement event (40). The preexisting *N. europaea* *AMT* gene was displaced (replaced) by the HGT-acquired *RH50*; it remains open to question whether this replacement has taken place via a loss-and-regain strategy (following consecutive and opposite adaptive selection pressures) or else the two genes have coexisted in *N. europaea* for a given time span (20). However, the presence of both *AMT* and *RH50* in the genomes of “*Ca. Kuenenia*” and *Acidobacteria* (see above) may favor the second hypothesis.

***RH50*_{Ne} mediates ammonium uptake and may thus have replaced *AMT* functionally.** The proposal of Soupene et al. (65) that Amt proteins act as NH₃ channels has been supported by X-ray crystal structures of *E. coli* AmtB (36, 83) and *Archaeoglobus fulgidus* Amt1 (3) and by in vivo studies on *E. coli* AmtB (32). However, studies on other Amt proteins (from *Corynebacterium glutamicum* or *Lycopersicon esculentum*) have suggested that they act as NH₄⁺ uniporters (47, 64).

The biochemical function(s) of Rh50 proteins is still a matter of debate. In vertebrates, where Amt proteins are absent, a series of studies, mainly in heterologous systems, has suggested that Rh50 proteins may act as ammonium transport proteins. Marini et al. provided the first evidence that human Rh50A and Rh50C can mediate ammonium uptake when expressed in yeast (49), and many subsequent reports have corroborated the function of the mammalian Rh50 proteins as ammonium transporters (33). Furthermore, in the pufferfish, *Takifugu rubripes*, the four Rh50 proteins mediate MA entry when expressed in *Xenopus* oocytes and are expressed in different cell types in the gills (54), the main site of ammonia excretion in aquatic animals, together with skin.

RH50 genes have also been studied in nonvertebrates: the slime mold *Dictyostelium discoideum* (7), the lepidopteran *Manduca sexta* (78), and the nematode *Caenorhabditis elegans* (35). The green alga *Chlamydomonas reinhardtii* has two *RH50* genes (*CrRH1* and *CrRH2*) and at least four *AMT* genes (37). Expression of both *CrRH1* mRNA and CrRh1 protein increase when the available CO₂ is increased from 0.035 to 3% (66), and RNA interference silencing of *CrRH1* correlated with growth defects when the mutant lines were grown at a high CO₂ concentration (67). These results led the authors to propose that Rh proteins might act as CO₂ channels in the green algae and also in mammals (66). However, while this hypothesis is plausible for *Chlamydomonas*, firm evidence has yet to be provided for its extension to Rh50 homologs in other species. The hypotheses on the function of Rh50 proteins, as ammonium or CO₂ channels (67) or as nonspecific channels for neutral small molecules (10) are of course not mutually exclusive since it is well known that homologous proteins may have the same functions, similar but also different functions, or multiple functions in different organisms (22).

In *N. europaea* ammonia appears to play a critical role serving as a signal leading to regulation of gene transcription (61, 75, 76), as a metabolic substrate, and as the sole energy source

for ammonia oxidation in aerobic conditions. Based on the *N. europaea* genome sequence, Chain et al. predicted that ammonium entry into the cell might occur via the Rh50 protein (13). However, evidence has also been provided for the existence in *N. europaea* of an active membrane-potential-driven transport mechanism (13), which might enable ammonium to reach an internal (cytoplasm plus periplasm) concentration as high as 1 M (62) and allow the organism to cope with the very low concentrations of ammonium present in the environment (8).

Our results indicate that the Rh50_{Ne} protein is involved in ammonium uptake; its depletion in the corresponding KO mutant results in an extended lag phase on low ammonium and in markedly reduced MA uptake compared to the wild type (Fig. 4). Modeling of the human Rh50A protein based on the X-ray crystal structure of the *E. coli* AmtB protein has shown that Rh50A is likely to adopt a structure similar to that of AmtB, and Rh50A is expected to have a channel architecture very similar to that of AmtB (11, 15). Indeed, we recently solved the X-ray crystal structure of Rh50_{Ne} (47a) and showed it to be a trimeric protein with a channel architecture very similar to that predicted by our previous homology modeling of Rh50A (15). Hence, Rh proteins appear to have many of the essential characteristics to facilitate ammonium uptake, and our empirical data with Rh50_{Ne} (Fig. 3 and 4) support this proposition.

Restoration of ammonium-dependent growth to a yeast Δ mep mutant by Rh50_{Ne} is more effective as the pH increases (Fig. 3), a result that is compatible either with facilitated transport of NH₃ through the channel or with a NH₄⁺/H⁺ exchanger. However, one feature of Amt proteins is a periplasmic vestibule that has been proposed to contain a binding site for the ammonium ion, defined by three conserved residues (Phe103, Trp148, and Ser219 in AmtB_{Ec}) (83). Rh50 proteins, including Rh50_{Ne}, lack all three residues (15, 47a), and if Rh50_{Ne} were functioning as an NH₃ channel, then the absence of this putative ammonium ion binding site would be consistent with the pH-dependent growth that we observe when Rh50_{Ne} is expressed in the yeast Δ mep mutant.

The failure of Rh50_{Ne} to mediate MA uptake is not unprecedented, and similar observations have been made with human Rh50A expressed in *S. cerevisiae* (49, 80). Although it is conceivable that at least some Rh50 proteins might mediate CO₂ uptake, our experiments to characterize Rh50_{Ne} in vivo showed no evidence of a CO₂-dependent growth effect in a *RH50*_{Ne}-KO mutant. Hence, we presently have no evidence that Rh50_{Ne} functions as a CO₂ channel.

Overall, we have provided evidence indicating that the Rh50 protein mediates ammonium uptake in *N. europaea* and thus may have replaced functionally a preexisting Amt protein (though the reasons for the loss of the *AMT* gene are unknown). It has been shown that ammonium is a crucial factor for the differentiation of the ecological niche of AOB (8). When the ammonium concentration in the environment is low, AOB, given their low growth rate, suffer badly from the competition of other microbes for energy sources. AOB appear to have developed a survival strategy at the molecular level by regulating transcription levels. Indeed, under starvation conditions (NH₃ plus CO₂ removal), while ca. 68% of *N. europaea* genes are downregulated (at least twofold) and ammonia monooxygenase and hydroxylamine oxidoreductase transcrip-

tion levels are maintained, 10 genes, mainly related to oxidative stress, are upregulated by more than twofold, and transcription of *RH50_{Ne}* increases nearly twofold (76). *Rh50_{Ne}* may therefore be a key player (as a channel and/or a sensor of ammonium) in the survival strategy of *N. europaea*, which has adapted to long periods of starvation while preparing for the uptake and the oxidation of ammonia as soon as it becomes available (8).

ACKNOWLEDGMENTS

G.M. expresses the warmest thanks to Dick D'Ari, without whom this work would not have been completed. B.C.-Z. thanks Aleksander Edelman for supporting this study. We thank Tim Fulford for helpful advice on the execution of the yeast experiments and for the construction of plasmid pTF14 and Jasmin Wickinghoff for excellent technical assistance. We thank Norman Hommes for the gift of *N. europaea* ATCC 19718 and the pRL448 plasmid and for technical advice and discussion. We thank Hervé Philippe for very helpful discussions and suggestions.

This work was supported by a grant from the Biotechnology and Biological Sciences Research Council to M.M. and A.D.

ADDENDUM

Evidence that *Rh50_{Ne}* mediates ammonia transport has also been provided by Weidinger et al. (77).

REFERENCES

- Abascal, F., R. Zardoya, and D. Posada. 2005. ProtTest: selection of bestfit models of protein evolution. *Bioinformatics* **21**:2104–2105.
- Altschul, S. F., T. L. Madden, A. A. Schäffer, J. Zhang, Z. Zhang, W. Miller, and D. J. Lipman. 1997. Gapped BLAST and PSI-BLAST: a new generation of protein database search programs. *Nucleic Acids Res.* **25**:3389–3402.
- Andrade, S. L., A. Dickmanns, R. Ficner, and O. Einsle. 2005. Crystal structure of the archaeal ammonium transporter Amt-1 from *Archaeoglobus fulgidus*. *Proc. Natl. Acad. Sci. USA* **102**:14994–14999.
- Anisimova, M., and O. Gascuel. 2006. Approximate likelihood-ratio test for branches: a fast, accurate, and powerful alternative. *Syst. Biol.* **55**:539–552.
- Arp, D. J., L. A. Sayavedra-Soto, and N. G. Hommes. 2002. Molecular biology and biochemistry of ammonia oxidation by *Nitrosomonas europaea*. *Arch. Microbiol.* **178**:250–255.
- Avent, N. D., and M. E. Reid. 2000. The Rh blood group system: a review. *Blood* **95**:375–387.
- Benghezal, M., D. Gotthardt, S. Cornillon, and P. Cosson. 2001. Localization of the Rh50-like protein to the contractile vacuole in *Dictyostelium*. *Immunogenetics* **52**:284–288.
- Bollmann, A., M. J. Bar-Gilissen, and H. J. Laanbroek. 2002. Growth at low ammonium concentrations and starvation response as potential factors involved in niche differentiation among ammonia-oxidizing bacteria. *Appl. Environ. Microbiol.* **68**:4751–4757.
- Bradford, M. 1976. Rapid and sensitive methods for the quantitation of microgram quantities of protein utilizing the principle of protein dye binding. *Anal. Biochem.* **72**:248–254.
- Bruce, L. J., R. Beckmann, M. L. Ribeiro, L. L. Peters, J. A. Chasis, J. Delaunay, N. Mohandas, D. J. Anstee, and M. J. Tanner. 2003. A band 3-based macrocomplex of integral and peripheral proteins in the RBC membrane. *Blood* **101**:4180–4188.
- Callebaut, I., F. Dulin, O. Bertrand, P. Ripoche, I. Mouro, Y. Colin, et al. 2006. Hydrophobic cluster analysis and modeling of the human Rh protein three-dimensional structures. *Transfusion Clin. Biol.* **13**:70–84.
- Castresana, J. 2000. Selection of conserved blocks from multiple alignments for their use in phylogenetic analysis. *Mol. Biol. Evol.* **17**:540–552.
- Chain, P., J. Lamerdin, F. Larimer, W. Regala, V. Lao, M. Land, et al. 2003. Complete genome sequence of the ammonia-oxidizing bacterium and obligate chemolithoautotroph *Nitrosomonas europaea*. *J. Bacteriol.* **185**:2759–2773.
- Cherif-Zahar, B., V. Raynal, P. Gane, M. G. Mattei, P. Bailly, B. Gibbs, Y. Colin, and J. P. Cartron. 1996. Candidate gene acting as a suppressor of the RH locus in most cases of Rh deficiency. *Nat. Genet.* **12**:168–173.
- Conroy, M. J., P. A. Bullough, M. Merrick, and N. D. Avent. 2005. Modelling the human rhesus proteins: implications for structure and function. *Br. J. Haematol.* **131**:543–551.
- Corpet, F. 1988. Multiple sequence alignment with hierarchical clustering. *Nucleic Acids Res.* **16**:10881–10890.
- Coutts, G., G. Thomas, D. Blakey, and M. Merrick. 2002. Membrane sequestration of the signal transduction protein GlnK by the ammonium transporter AmtB. *EMBO J.* **21**:536–545.
- Datsenko, K. A., and B. L. Wanner. 2000. One-step inactivation of chromosomal genes in *Escherichia coli* K-12 using PCR products. *Proc. Natl. Acad. Sci. USA* **97**:6640–6645.
- Dimmic, M. W., J. S. Rest, D. P. Mindell, and R. A. Goldstein. 2002. rtREV: an amino acid substitution matrix for inference of retrovirus and reverse transcriptase phylogeny. *J. Mol. Evol.* **55**:65–73.
- Doolittle, W. F., Y. Boucher, C. L. Nesbo, C. J. Douady, J. O. Andersson, and A. J. Roger. 2003. How big is the iceberg of which organellar genes in nuclear genomes are but the tip? *Philos. Trans. R. Soc. London B Biol. Sci.* **358**:39–57.
- Elhai, J., and C. P. Wolk. 1988. A versatile class of positive-selection vectors based on the nonviability of palindrome-containing plasmids that allows cloning into long polylinkers. *Gene* **68**:119–138.
- Fitch, W. T. 2000. Homology a personal view on some of the problems. *Trends Genet.* **16**:227–231.
- Galtier, N., M. Gouy, and C. Gautier. 1996. SeaView and Phylo_win, two graphic tools for sequence alignment and molecular phylogeny. *Comput. Appl. Biosci.* **12**:543–548.
- Guindon, S., and O. Gascuel. 2003. A simple, fast, and accurate algorithm to estimate large phylogenies by maximum likelihood. *Syst. Biol.* **52**:696–704.
- Gupta, R. S., and P. H. A. Sneath. 2007. Application of the character compatibility approach to generalized molecular sequence data: branching order of the proteobacterial subdivisions. *J. Mol. Evol.* **64**:90–100.
- Hasegawa, M., H. Kishino, and T. Yano. 1985. Dating of the human-ape splitting by a molecular clock of mitochondrial DNA. *J. Mol. Evol.* **22**:160–174.
- Henikoff, S., and J. G. Henikoff. 1992. Amino acid substitution matrices from protein blocks. *Proc. Natl. Acad. Sci. USA* **89**:10915–10919.
- Hommes, N. G., L. A. Sayavedra-Soto, and D. J. Arp. 1996. Mutagenesis of hydroxylamine oxidoreductase in *Nitrosomonas europaea* by transformation and recombination. *J. Bacteriol.* **178**:3710–3714.
- Hyman, M. R., and D. J. Arp. 1992. ¹⁴C₂H₂- and ¹⁴CO₂-labeling studies of the de novo synthesis of polypeptides by *Nitrosomonas europaea* during recovery from acetylene and light inactivation of ammonia monooxygenase. *J. Biol. Chem.* **267**:1534–1545.
- Javelle, A., E. Severi, J. Thornton, and M. Merrick. 2004. Ammonium sensing in *Escherichia coli*: the role of the ammonium transporter AmtB and AmtB-GlnK complex formation. *J. Biol. Chem.* **279**:8530–8538.
- Javelle, A., D. Lupo, L. Zheng, X. D. Li, F. K. Winkler, and M. Merrick. 2006. An unusual twin-His arrangement in the pore of ammonia channels is essential for substrate conductance. *J. Biol. Chem.* **281**:39492–39498.
- Javelle, A., G. Thomas, A. M. Marini, R. Kramer, and M. Merrick. 2005. In vivo functional characterisation of the *Escherichia coli* ammonium channel AmtB: evidence for metabolic coupling of AmtB to glutamine synthetase. *Biochem. J.* **390**:215–222.
- Javelle, A., D. Lupo, X. D. Li, M. Merrick, M. Chami, P. Ripoche, and F. K. Winkler. 2007. Structural and mechanistic aspects of Amt/Rh proteins. *J. Struct. Biol.* **158**:472–481.
- Jenkins, C., R. Samudrala, I. Anderson, B. P. Hedlund, G. Petroni, N. Michailova, et al. 2002. Genes for the cytoskeletal protein tubulin in the bacterial genus *Prostheco bacter*. *Proc. Natl. Acad. Sci. USA* **99**:17049–17054.
- Ji, Q., S. Hashmi, Z. Liu, J. Zhang, Y. Chen, and C. H. Huang. 2006. CeRh1 (rhr-1) is a dominant Rhesus gene essential for embryonic development and hypodermal function in *Caenorhabditis elegans*. *Proc. Natl. Acad. Sci. USA* **103**:5881–5886.
- Khademi, S., J. O'Connell III, J. Remis, Y. Robles-Colmenares, L. J. Miercke, and R. M. Stroud. 2004. Mechanism of ammonia transport by Amt/MEP/Rh: structure of AmtB at 1.35 Å. *Science* **305**:1587–1594.
- Kim, K.-S., E. Field, N. King, T. Yaoi, S. Kustu, and W. Inwood. 2005. Spontaneous mutations in the ammonium transport gene AMT4 of *Chlamydomonas reinhardtii*. *Genetics* **170**:631–644.
- Kitano, T., K. Sumiyama, T. Shiroishi, and N. Saitou. 1998. Conserved evolution of the Rh50 gene compared to its homologous Rh blood group gene. *Biochem. Biophys. Res. Commun.* **249**:78–85.
- Kitano, T., and N. Saitou. 2000. Evolutionary history of the Rh blood group-related genes in vertebrates. *Immunogenetics* **51**:856–862.
- Koonin, E. V., A. R. Mushegian, and P. Bork. 1996. Non-orthologous gene displacement. *Trends Genet.* **12**:334–336.
- Koonin, E. V., K. S. Makarova, and L. Aravind. 2001. Horizontal gene transfer in prokaryotes: quantification and classification. *Annu. Rev. Microbiol.* **55**:709–742.
- Koonin, E. V. 2005. Orthologs, paralogs, and evolutionary genomics. *Annu. Rev. Genet.* **39**:309–338.
- Kustu, S., and W. Inwood. 2006. Biological gas channels for NH₃ and CO₂: evidence that Rh (Rhesus) proteins are CO₂ channels. *Transfusion Clin. Biol.* **13**:103–110.
- Lanave, C., G. Preparata, C. Saccone, and G. Serio. 1984. A new method for calculating evolutionary substitution rates. *J. Mol. Evol.* **20**:86–93.
- Landsteiner, K., and A. S. Wiener. 1940. An agglutinable factor in human

- blood recognized by immune sera for rhesus blood. *Proc. Soc. Exp. Biol. Med.* **43**:223–224.
46. Leon, G., and P. H. Roy. 2003. Excision and integration of cassettes by an integrin integrase of *Nitrosomonas europaea*. *J. Bacteriol.* **185**:2036–2041.
 47. Ludewig, N. U., von Wirén, and W. B. Frommer. 2002. Uniport of NH_4^+ by the root hair plasma membrane ammonium transporter LeAMT1;1. *J. Biol. Chem.* **277**:13548–13555.
 - 47a. Lupo, D., X.-D. Li, A. Durand, T. Tomizaki, B. Cherif-Zahar, G. Matassi, M. Merrick, and F. K. Winkler. The 1.3 Å resolution structure of *Nitrosomonas europaea* Rh50 and mechanistic implications for NH_3 transport by Rhesus family proteins. *Proc. Natl. Acad. Sci. USA*, in press.
 48. Marini, A. M., A. Urrestarazu, R. Beauwens, and B. Andre. 1997. The Rh (rhesus) blood group polypeptides are related to NH_4^+ transporters. *Trends Biochem. Sci.* **22**:460–461.
 49. Marini, A. M., G. Matassi, V. Raynal, B. Andre, J. P. Cartron, and B. Cherif-Zahar. 2000. The human Rhesus-associated RhAG protein and a kidney homologue promote ammonium transport in yeast. *Nat. Genet.* **26**:341–344.
 50. Marini, A. M., S. Soussi-Boudekou, S. Vissers, and B. Andre. 1997. A family of ammonium transporters in *Saccharomyces cerevisiae*. *Mol. Cell. Biol.* **17**:4282–4293.
 51. Marino, R., D. Melillo, M. Di Filippo, A. Yamada, M. R. Pinto, R. De Santis, E. R. Brown, and G. Matassi. 2007. Ammonium channel expression is essential for brain development and function in the larva of *Ciona intestinalis*. *J. Comp. Neurol.* **503**:135–147.
 52. Matassi, G., B. Cherif-Zahar, G. Pesole, V. Raynal, and J. P. Cartron. 1999. The members of the RH gene family (RH50 and RH30) underwent different evolutionary pathways. *J. Mol. Evol.* **48**:151–159.
 53. Matassi, G., B. Cherif-Zahar, V. Raynal, P. Rouger, and J. P. Cartron. 1998. Organization of the human RH50A gene (RHAG) and evolution of base composition of the RH gene family. *Genomics* **47**:286–293.
 54. Nakada, T., C. M. Westhoff, A. Kato, and S. Hirose. 2007. Ammonia secretion from fish gill depends on a set of Rh glycoproteins. *FASEB J.* **21**:1067–1074.
 55. Notredame, C., D. Higgins, and J. Heringa. 2000. T-Coffee: a novel method for multiple sequence alignments. *J. Mol. Biol.* **302**:205–217.
 56. Ochman, H., J. G. Lawrence, and E. A. Groisman. 2000. Lateral gene transfer and the nature of bacterial innovation. *Nature* **405**:299–304.
 57. Purkhold, U., A. Pommerening-Roser, S. Juretschko, M. C. Schmid, H.-P. Koops, and M. Wagner. 2000. Phylogeny of all recognized species of ammonia oxidizers based on comparative 16S rRNA and *amoA* sequence analysis: implications for molecular diversity surveys. *Appl. Environ. Microbiol.* **66**:5368–5382.
 58. Purkhold, U., M. Wagner, G. Timmermann, A. Pommerening-Roser, and H.-P. Koops. 2003. 16S rRNA and *amoA*-based phylogeny of 12 novel betaproteobacterial ammonia-oxidizing isolates: extension of the dataset and proposal of a new lineage within the nitrosomonads. *Int. J. Syst. Evol. Microbiol.* **53**:1485–1494.
 59. Rentsch, D., M. Laloi, I. Rouhara, E. Scmelzer, S. Delrot, and W. B. Frommer. 1995. NTR1 encodes a high-affinity oligopeptide transporter in *Arabidopsis*. *FEBS Lett.* **370**:264–268.
 60. Rowe-Magnus, D. A., and D. Mazel. 2001. Integrons: natural tools for bacterial genome evolution. *Curr. Opin. Microbiol.* **4**:565–569.
 61. Sayavedra-Soto, L. A., N. G. Hommes, S. A. Russell, and D. J. Arp. 1996. Induction of ammonia monoxygenase and hydroxylamine oxidoreductase mRNAs by ammonium in *Nitrosomonas europaea*. *Mol. Microbiol.* **20**:541–548.
 62. Schmidt, I., C. Look, E. Bock, and M. S. Jetten. 2004. Ammonium and hydroxylamine uptake and accumulation in *Nitrosomonas*. *Microbiology* **150**:1405–1412.
 63. Schmidt, I., and E. Bock. 1997. Anaerobic ammonia oxidation with nitrogen dioxide by *Nitrosomonas europaea*. *Arch. Microbiol.* **167**:106–111.
 64. Siewe, R. M., B. Weil, A. Burkovski, B. J. Eikmanns, M. Eikmanns, and R. Krämer. 1996. Functional and genetic characterisation of the (methyl)ammonium uptake carrier of *Corynebacterium glutamicum*. *J. Biol. Chem.* **271**:5398–5403.
 65. Soupene, E., R. M. Ramirez, and S. Kustu. 2001. Evidence that fungal MEP proteins mediate diffusion of the uncharged species NH_3 across the cytoplasmic membrane. *Mol. Cell. Biol.* **21**:5733–5741.
 66. Soupene, E., N. King, E. Field, P. Liu, K. K. Niyogi, C. H. Huang, and S. Kustu. 2002. Rhesus expression in a green alga is regulated by CO_2 . *Proc. Natl. Acad. Sci. USA* **99**:7769–7773.
 67. Soupene, E., W. Inwood, and S. Kustu. 2004. Lack of the Rhesus protein Rh1 impairs growth of the green alga *Chlamydomonas reinhardtii* at high CO_2 . *Proc. Natl. Acad. Sci. USA* **101**:7787–7792.
 68. Sturgeon, P. 1970. Hematological observations on the anemia associated with blood type Rhnull. *Blood* **36**:310–320.
 69. Suyama, M., D. Torrents, and P. Bork. 2006. PAL2NAL: robust conversion of protein sequence alignments into the corresponding codon alignments. *Nucleic Acids Res.* **34**:W609–W612.
 70. Syvanen, M. 1994. Horizontal gene transfer: evidence and possible consequences. *Annu. Rev. Genet.* **28**:237–261.
 71. Teeling, H., and F. O. Gloeckner. 2006. RibAlign: a software tool and database for eubacterial phylogeny based on concatenated ribosomal protein subunits. *BMC Bioinform.* **7**:66–71.
 72. Thomas, G. H., J. G. Mullins, and M. Merrick. 2000. Membrane topology of the Mep/Amt family of ammonium transporters. *Mol. Microbiol.* **37**:331–344.
 73. van de Graaf, A. A., P. de Bruijn, L. A. Robertson, and J. G. Kuenen. 1996. Autotrophic growth of anaerobic ammonium-oxidizing micro-organisms in a fluidized bed reactor. *Microbiology* **142**:2187–2196.
 74. von Wirén, N., and M. Merrick. 2004. Regulation and function of ammonium carriers in bacteria, fungi and plants. *Trends Curr. Genet.* **9**:95–120.
 75. Wei, X., L. A. Sayavedra-Soto, and D. J. Arp. 2004. The transcription of the *cbb* operon in *Nitrosomonas europaea*. *Microbiology* **150**:1869–1879.
 76. Wei, X., T. Yan, N. G. Hommes, X. Liu, L. Wu, C. McAlvin, et al. 2006. Transcript profiles of *Nitrosomonas europaea* during growth and upon deprivation of ammonia and carbonate. *FEMS Microbiol. Lett.* **257**:76–83.
 77. Weidinger, K., B. Neuhauser, S. Gilch, U. Ludewig, O. Meyer, and I. Schmidt. 2007. Functional and physiological evidence for a rhesus-type ammonia transporter in *Nitrosomonas europaea*. *FEMS Microbiol. Lett.* **273**:260–267.
 78. Weihrauch, D. 2006. Active ammonia absorption in the midgut of the tobacco hornworm *Manduca sexta* L.: transport studies and mRNA expression analysis of a Rhesus-like ammonia transporter. *Insect Biochem. Mol. Biol.* **36**:808–821.
 79. Weiner, I. D., and L. L. Hamm. 2007. Molecular mechanisms of renal ammonia transport. *Annu. Rev. Physiol.* **69**:317–340.
 80. Westhoff, C. M., D. L. Siegel, C. G. Burd, and J. K. Foskett. 2004. Mechanism of genetic complementation of ammonium transport in yeast by human erythrocyte Rh-associated glycoprotein. *J. Biol. Chem.* **279**:17443–17448.
 81. Whelan, S., and N. Goldman. 2001. A general empirical model of protein evolution derived from multiple protein families using a maximum-likelihood approach. *Mol. Biol. Evol.* **18**:6.
 82. Winkler, F. K. 2006. Amt/MEP/Rh proteins conduct ammonia. *Pflügers Arch.* **451**:701–707.
 83. Zheng, L., D. Kostrewa, S. Bernèche, F. K. Winkler, and X.-D. Li. 2004. The mechanism of ammonia transport based on the crystal structure of AmtB of *Escherichia coli*. *Proc. Natl. Acad. Sci. USA* **101**:17090–17095.